Cohesive and magnetic properties of Ni, Co, and Fe on W(100), (110), and (111) surfaces: A first-principles study

S. F. Huang,[1] R. S. Chang,[1] T. C. Leung,[1,2] and C. T. Chan[3]
[1]*Department of Physics, National Chung Cheng University, Chia-Yi, Taiwan, Republic of China*
[2]*Center for Nanotechnology Design and Proptotyping, National Chung Cheng University, Chia-Yi, Taiwan, Republic of China*
[3]*Physics Department, Hong Kong University of Science and Technology, Clear Water Bay, Hong Kong, China*
(Received 20 April 2005; published 22 August 2005)

Local density functional calculations are used to investigate the structural, cohesive, and magnetic properties of Ni, Co, and Fe on various orientations of the W surface. We found that all these elements wet all the W surface orientations for at least one monolayer so that thermodynamically stable ultrathin coatings of these elements can be formed. However, the magnetic properties are strongly orientation dependent. We will see that thermodynamically stable and ferromagnetic ultrathin coatings with large differences between the majority- and minority-spin density of states near the Fermi level may be realizable for some of these 3*d* metals on some orientations of the tungsten surface.

DOI: 10.1103/PhysRevB.72.075433 PACS number(s): 75.70.−i, 71.15.Nc, 71.15.Mb, 73.30.+y

I. INTRODUCTION

The magnetism and other physical properties of ultrathin magnetic layers have attracted a lot of attention from theorists and experimentalists,[1–4] not just because of their fundamental importance as a physics problem, but also because of many plausible applications.[5] In this paper, we report some theoretical calculations that address the properties of thin magnetic layers grown on top of various orientations of the W surface. Instead of focusing on one single system, we investigated and compared the energetics and surface magnetisms of three 3*d* elements on three different orientations of the refractory metal substrate. This comprehensive study establishes a systematic trend of behavior and offers us a better feeling of the physics governing the thermodynamics and magnetic properties of ultrathin magnetic films on refractory metal surfaces. These studies also shed some light on whether these systems may be used a source of spin-polarized electrons in field emission.[6] We note that while refractory metals are frequently employed as field emission tips, they cannot be used as spin-polarized electron sources since they are not magnetic. However, refractory metal tips coated with a thin layer of magnetic film may have the potential of being developed into a source of spin-polarized electrons. That requires that the coating layer be stable, be magnetic, and have a significant difference between the majority- and minority-spin density of states near the Fermi level. We will see that ultrathin films of some 3*d* metals on W surfaces can satisfy these necessary conditions.

II. METHOD OF CALCULATION

The calculations are performed using the computer program WIEN2k,[7] an implementation of the full-potential linear augmented plane-wave method[8] (FLAPW) based on density functional theory.[9] For the exchange and correlation potential we used the Perdew-Burke-Ernzerhof (PBE) generalized gradient approximation (GGA) form.[10] The scalar relativistic treatment including the velocity and Darwin terms was adopted in our calculation. Spin-orbit coupling was not included; therefore, the orbital magnetic moment is not calculated. The magnitude of the orbital magnetic moment was estimated to be around $0.1\mu_B$.[11] We used the repeated geometry to model the surface systems. The W substrates are modeled by 5- and 7-layer slabs for the W(100) and W(110) orientations, and 7- and 11-layer slabs are used for W(111). The surface unit cell is $p(1\times1)$, and therefore we have restricted ourselves to ferromagnetic states of the magnetic film. Since we are looking for thin-film magnetism, the coating layer elements are chosen to be elements like Ni, Co, and Fe, which are magnetic in the bulk. The coating overlayers are pseudomorphoic and are put on both sides of the substrate W slab. The vacuum thickness is 10 Å. All atomic coordinates are fully relaxed. The atomic relaxation is important since surface magnetism is rather sensitive to the interlayer distance between the overlayer and substrate. For the (100) and (110) orientations, we have considered overlayer thicknesses of one and two monolayers, while for the (111) orientation, we have considered the adsorption of one, two, and three monolayers. The *k*-point sampling is $16\times16\times1$ for (100) and (110) orientations and $12\times12\times1$ for (111) orientation. The radius of the muffin tin is 2.3 a.u. for W atoms and 2.0 a.u. for Fe, Co, and Ni atoms. A plane-wave cutoff energy of 16 Ry and convergence criteria for energy of 10^{-5} Ry are selected. All the interlayer distances were fully relaxed by computing the Hellmann-Feynmann forces, until the maximum force acting on the atoms was smaller than 5 mRy/a.u. As a test, calculations with various vacuum thicknesses, plane-wave cutoff energies, and *k*-point sampling were performed and magnetic moments are found to converge to $0.1\mu_B$ and the heat of formation is converged to 0.01 eV.

III. RESULTS

Our results are summarized in Table I, in which we list the magnetic moments (in μ_B) of the coating layer atoms and the heat of formation of the overlayer. Results are shown for

TABLE I. Magnetic moment and heat of formation. Here, a negative value of the heat of formation means stable adsorption.

	Magnetic moment (μ_B)				
	Overlayers			W	Heat of formation (eV)
1Fe/5W(100)			1.89	−0.22	−0.61
1Fe/7W(100)			1.78	−0.20	−0.57
2Fe/5W(100)		2.73	1.90	−0.23	0.00
2Fe/7W(100)		2.75	1.92	−0.21	0.01
1Co/5W(100)			0.09	0.00	−0.72
1Co/7W(100)			0.06	0.00	−0.70
2Co/5W(100)		1.75	1.51	0.01	0.22
2Co/7W(100)		1.73	1.49	0.02	0.25
1Ni/5W(100)			0.00	0.00	−0.86
1Ni/7W(100)			0.00	0.00	−0.82
2Ni/5W(100)		0.00	0.00	0.00	−0.15
2Ni/7W(100)		0.00	0.00	0.00	−0.13
1Fe/5W(110)			2.45	−0.10	−0.23
1Fe/7W(110)			2.46	−0.09	−0.22
2Fe/5W(110)		2.80	2.29	−0.10	0.01
2Fe/7W(110)		2.81	2.28	−0.09	0.00
1Co/5W(110)			1.40	−0.03	−0.08
1Co/7W(110)			1.51	0.00	−0.03
2Co/5W(110)		2.02	1.69	0.01	0.30
2Co/7W(110)		2.01	1.69	0.03	0.31
1Ni/5W(110)			0.00	0.00	−0.38
1Ni/7W(110)			0.00	0.00	−0.38
2Ni/5W(110)		0.71	0.14	−0.02	0.44
2Ni/7W(110)		0.79	0.20	0.00	0.45
1Fe/7W(111)			2.30	−0.30	−0.53
1Fe/11W(111)			2.10	−0.24	−0.47
2Fe/7W(111)		2.73	2.06	−0.16	−0.18
2Fe/11W(111)		2.73	1.81	−0.22	−0.09
3Fe/7W(111)	2.72	2.60	2.52	−0.14	0.37
3Fe/11W(111)	2.71	2.58	2.50	−0.15	0.38
1Co/7W(111)			1.23	−0.05	−0.49
1Co/11W(111)			0.76	−0.04	−0.44
2Co/7W(111)		1.69	1.05	−0.01	0.02
2Co/11W(111)		1.69	0.79	−0.03	0.08
3Co/7W(111)	1.68	1.88	1.51	0.02	0.59
3Co/11W(111)	1.65	1.84	1.47	0.01	0.64
1Ni/7W(111)			0.00	0.00	−0.79
1Ni/11W(111)			0.00	0.00	−0.74
2Ni/7W(111)		.00	0.00	0.00	−0.21
2Ni/11W(111)		0.00	0.00	0.00	−0.20
3Ni/7W(111)	0.43	0.43	0.18	0.10	0.40
3Ni/11W(111)	0.40	0.37	0.15	0.09	0.43

one and two monolayers of Fe, Co, and Ni on the (100) and (110) orientations and from one to three monolayers on the (111) orientation. In our calculations, the heat of formation per overlayer atom is defined as

$$\frac{1}{2}(E_{(slab+overlayer)} - E_{slab} - 2E_{bulk}), \quad (1)$$

where $E_{(slab+overlayer)}$ is the total energy of the slab plus an additional two-dimensional (2D) pseudomorphoic overlayer of Fe, Co, or Ni covering either side the substrate slab. E_{slab} is the energy of the slab without the overlayer, and E_{bulk} is the energy of the overlayer element in the bulk environment. There is a factor of 2 that premultiplies the E_{bulk} because we are putting overlayers on both side of the slab in a (1×1) surface unit cell so that we are adding two overlayer atoms to the supercell for every monolayer that is added to one side of the slab. Similarly, the factor of $\frac{1}{2}$ is to account for the fact that we have two surfaces in our symmetric slab geometric. The heat of formation defined this manner basically compares the energy of two systems: (i) the overlayer forming a 2D pseudomophic layer coating the substrate and (ii) the overlayer elements clump up to form a 3D macroscopic island of its own, leaving the substrate exposed to vacuum. If the former has lower energy than the latter ($H<0$), the overlayer will wet the substrate. By computing this heat of formation for each additional overlayer and monitoring when this number goes positive, we can tell when the growth mode would change from layer by layer to 3D island formation. From the values shown in Table I, we see that one monolayer of all three $3d$ metals wets the W substrate for all three orientations we considered. The heat of formation is less than 0.4 eV for the (110) orientation and somewhat higher for the more open (100) and (111) orientations. This is consistent with the high surface energy of W. W does not want to expose its atoms to the vacuum, and the surface energy becomes lower when the surface is covered by $3d$ metal atoms which have lower surface energies. For the absorption of the second layer on both the (110) and (100) orientations, the heat of formation either becomes positive or just slightly negative. This means that in the more compact surface orientations, the first layer already shields the second layer from bonding with the W substrate. For the (111) orientation, both the first and second layers of Fe and Ni wet the W substrate. It is because the (111) orientation is rougher and more open than the other two orientations. Summarizing, we see that these magnetic $3d$ metals wet the W surface at different orientations with at least one monolayer to form thermodynamically stable films. It is of course possible to form thicker overlayer films that are metastable if the deposition is carried out at lower temperatures.

The surface magnetic properties of these overlayers are also shown in Table I. We show the magnetic moments, in Bohr magneton units (μ_B), for the overlayer atoms and the top layer of the W substrate. From Table I, we observe some obvious trends. First, the magnetic moments for the same thickness and orientation are always going in the order Fe $>$Co$>$Ni. This agrees with the trend in bulk magnetism of these elements. The calculated magnetic moments for bulk Fe, Co, and Ni are 2.27, 1.70, and 0.62, respectively, in good agreement with the experimental values of 2.22, 1.72, and 0.61. The results for relaxed atomic geometries for Fe, Co, and Ni on W surfaces are shown in Table II. The relaxations of the interlayer spacings are stated with respect to the interlayer distances of bulk W(001), W(110), and W(111) layer spacings, respectively, where Δd_0 is the relaxation of the interface layer spacing between adatom and W and Δd_n and Δd_{-n} are for the layer spacings that are n layers away from interface in the adatom film and W substrate, respectively. For the case of Fe on W(110), our results are in good agreement with the previous calculations[12] and the experimental data.[13]

We see that the first and second Ni monolayers on W(100) and (111) and the first monolayer of Ni/W(110) have no magnetic moments. This is consistent with the weaker bulk magnetism of Ni. Another important factor is the higher cohesive energy of Ni on the W surface than the other two elements, indicating a stronger interaction and hybridization between the Ni and W orbitals. This shows that the proximity effect of the substrate is important and can make thin overlayers magnetically dead if the binding is strong between the overlayer elements and the substrate. The only case that Ni is magnetic on W is for two layers on top of W(110) and three layers on top of W(111). In these cases, we note that the heat of formation is already positive, which means that they are only thermodynamically metastable. If this configuration can be realized at low temperatures, the Ni film is ferromagnetic. The very fact that the heat of formation of the second layer is positive implies that the first Ni layer already shields the second Ni layer from bonding with the W substrate. It is not then surprising that the second layer becomes magnetic. When we compare the three orientations, we see that X/W(110) (X=Fe,Co,Ni) has consistently higher moments than X/W(100) and X/W(111). This correlates well with the trend in cohesive energies: X/(100) has highest binding in all cases, which signifies a stronger interaction, while (110) has the smallest. For all three elements we have considered, the interlayer separation between the overlayer and top layer of the (110) substrate is about 4.3 a.u., considerably larger than the corresponding distances of the other two orientations.

We also note that if the substrate is covered by two monolayers, the magnetic moments of the top overlayer atoms are in many cases bigger than that in the bulk of the $3d$ element. This is not surprising because of the reduced coordination in the surface environment. The $3d$ elements also have typically smaller atomic radii than the $5d$ W and are thus in a kind of expanded volume environment in pseudomorphoic films.

We note that the first monolayer of Co on W(100) has small magnetic moments. On the other hand, the magnetic moments of the first monolayer of Co on W(110) and W(111) are considerably larger. It implies that the interaction and hybridization between Co and W substrate are stronger for Co/W(100) than Co/W(110) and Co/W(111). This agrees with the stronger contraction of the interface layer spacing as well as the higher heat of formation in Co/W(100). Surface atoms usually have a larger magnetic moment relative to that in the bulk phase. This is indeed the case for almost all systems shown in the table. An exception is found in the case

TABLE II. The relaxed atomic geometries and the work functions for Fe, Co, and Ni on W surfaces.

	Relaxation (%)								Work function (eV)
				Δd_2	Δd_1	Δd_0	Δd_{-1}	Δd_{-2}	Φ
7W(100)						−10.7	2.2	−0.5	4.10
1Fe/7W(100)					−24.0	2.6	0.0	0.5	4.53
2Fe/7W(100)				−27.8	−12.1	0.6	−0.2	0.4	3.80
1Co/7W(100)					−33.5	2.2	−0.2	0.7	4.93
2Co/7W(100)				−37.8	−10.1	0.3	0.9	0.8	4.23
1Ni/7W(100)					−23.2	−2.0	1.5	0.2	4.97
2Ni/7W(100)				−27.3	−22.1	0.4	1.7	−0.3	4.10
				Δd_2	Δd_1	Δd_0	Δd_{-1}	Δd_{-2}	Φ
7W(110)						−2.5	0.9	0.4	4.79
1Fe/7W(110)					−12.1	0.9	0.5	1.3	4.26
2Fe/7W(110)				−20.9	−9.4	0.3	0.8	1.0	4.20
1Co/7W(110)					−14.8	1.5	0.8	1.1	4.31
2Co/7W(110)				−24.9	−8.9	0.7	1.5	2.0	4.28
1Ni/7W(110)					−16.8	1.1	0.5	0.8	4.26
2Ni/7W(110)				−22.0	−14.9	0.6	0.9	0.8	4.80
	Δd_2	Δd_1	Δd_0	Δd_{-1}	Δd_{-2}	Δd_{-3}	Δd_{-4}	Δd_{-5}	Φ
11W(111)				−21.1	−24.0	17.6	−4.3	3.2	4.25
1Fe/11W(111)			−32.3	−14.6	5.5	−3.9	3.5	1.9	4.33
2Fe/11W(111)		−13.4	−43.7	16.9	−4.9	−1.3	5.6	−0.1	4.25
3Fe/11W(111)	−14.3	−23.7	−5.3	−0.1	−1.8	2.7	0.9	−0.3	3.71
1Co/11W(111)			−40.8	−10.8	3.4	−4.5	6.2	1.6	4.39
2Co/11W(111)		−8.5	−52.2	18.4	−3.2	−2.6	4.9	−0.5	4.32
3Co/11W(111)	−27.7	−12.5	−11.5	−4.5	1.2	1.5	1.4	−0.4	4.14
1Ni/11W(111)			−36.5	−11.6	4.6	−5.9	6.1	1.3	4.39
2Ni/11W(111)		−12.2	−50.7	16.5	−0.2	−6.8	7.5	−0.6	4.52
3Ni/11W(111)	−20.3	−9.1	−22.0	−1.1	2.4	−0.6	3.4	0.0	4.17

of 3Co/W(111), in which the magnetic moment of the Co atom on the top layer is smaller than that of the second layer. These unexpected features can be correlated with the interlayer spacing relaxations. We list the interlayer spacings in Table II, and D_3, D_2, and D_1 are given by 0.67, 0.81, and 0.82 Å, respectively, for 3Co/W(111). For comparison, the interlayer spacings D_3, D_2, and D_1 are given by 0.79, 0.70, and 0.87 Å, respectively, for 3Fe/W(111). The interlayer distance between the first and second layers for 3Co/W(111) is smaller than that of 3Fe/W(111), and the interlayer distance between the second and third layers of 3Co/W(111) is larger than that of 3Fe/W(111). It correlates with the fact that the magnetic moment of the Co atom on the top layer is smaller than that of the second layer for the case 3Co/W(111) and the magnetic moment of the Fe atom on the top layer is larger than that of the second layer for the case of 3Fe/W(111). To check the result, we did the calculation using the projector augmented wave (PAW) method[14] as implemented in the VASP package[15] with PBE exchange-correlation potentials for 3Co/W(111). The results are very similar to that calculated using FLAPW with PBE potentials.

One useful property that can be derived immediately from the electronic structure calculations is the work function. The work function is determined from the difference between the Fermi level and the average potential in the vacuum region where it approaches a constant. The calculated work functions (based on PBE exchange correlation) for Fe, Co, and Ni on W surfaces are also shown in Table II. For clean surfaces, the (111) orientation has a relatively low work function which agrees with experimental findings. It is generally believed that the effect of a layer of adsorbates on the work function of a surface is governed by the electronegativity of the adsorbate. If the adsorbate is more electronegative than the substrate, the work function of the substrate increases. On the contrary, a decrease in work function is expected for electropositive adsorbates. As Fe, Co, and Ni are more electronegative than W on the Pauling scale, they should increase the work function of all W surfaces. However, the first layer of these metals increases the work function on (100) and (111) but decrease the work function on (110) as shown in Table II. The reason for the failure of the simple electronegativity argument has been discussed by a previous study,[16] which shows that the work function changes are not just

TABLE III. The work functions of clean W surfaces and one monolayer of Fe on W surfaces calculated using various methods. We note that while the values of the work function do depend on whether the GGA (with PBE) or LDA is used (the GGA consistently gives lower values of the work function than the LDA), the effect of the overlayer on the work function is very consistent.

	Work function (eV)			
	Expt.[a]	WIEN2k (PBE)	VASP (PAW-LDA)	VASP (PAW-PBE)
7W(100)	4.65	4.10	4.44	4.13
1Fe/7W(100)		4.53	4.77	4.49
7W(110)	5.25	4.79	5.07	4.84
1Fe/7W(110)		4.26	4.57	4.20
11W(111)	4.47	4.25	4.48	4.20
1Fe/11W(111)		4.33	4.69	4.31

[a]Reference 13.

decided by the value of charge transferred, but also by the details of the charge redistribution leading to a strong dependence of the work function change on the orientation of the substrate. The second overlayer may increase or decrease the work function, and such a strong oscillation of physical properties (quantum size effect) is rather common in ultrathin layers. Since the values of the work function depend on the details on the charge density, we also check some of our results using different exchange-correlation potentials and basis functions. For comparison, Table III shows the work function of clean W surfaces and one monolayer of Fe on W surfaces calculated using PAW (Ref. 15) with local density approximation (LDA) exchange correlation potentials, PAW with PBE exchange correlation potentials, and FLAPW with PBE. The experimental results of the clean surfaces are also shown[17] for reference. The work functions calculated by FLAPW (WIEN2k) and PAW with PBE potential agree very well with each other. The values of the work function calculated by PBE is always lower than the LDA, but the effect of the overlayer on the work function given by the LDA and PBE approximation are very consistent. It is clear that the LDA gives a better agreement with experiment than the PBE approximation.

In order to better understand the proximity effect of the substrate on the thin-film magnetism, we have calculated the magnetic moment of the overlayer atoms as we pull the overlayer away from the W substrate, with the substrate atoms at frozen positions. Table IV compares the magnetic moments of the first monolayer at their equilibrium positions (lowest-energy position) with the moments when the layer is pulled up into the vacuum by 0.5 and 1 Å. In each case, the moment increases as the overlayer is pulled away from the nonmagnetic substrate, as expected. The case of Ni clearly illustrates the quenching effect of the substrate. The Ni layers are magnetic when they are 1 Å above its lowest-energy position. We note that the packing densities of the monolayers at the three different orientations are different, and hence the magnetic moments can be different. For all three orientations, the moment becomes zero when the layer reaches the equilibrium position. By comparing the moment at 0.5 Å with those at 0 and 1 Å away from the equilibrium for Ni, we see that the quenching effect of the substrate goes in the order $(100)>(111)>(110)$, in the same order as the heat of formation. For Fe and Co, a single overlayer is magnetic at the equilibrium position (labeled as 0 Å in the table), and we see that the overlayer magnetic moment is smallest for the (100) orientation and highest for the (110) orientation. And hence the quenching effect for the substrate also goes in the order $(100)>(111)>(110)$, similar to the case of Ni. For these two elements, the magnetic moments of the 2D overlayers at different orientations are rather similar when the layers are about 1 Å away from their lowest-energy positions, but they become very different at the equilibrium position. This shows that the orientation dependence is mainly due to the overlayer-substrate interaction, rather than the interaction among the overlayer atoms.

To see the trend in the surface magnetism, we compare the spin-decomposed local density of states (LDOS) of the overlayer atoms. In LDOS calculations, we use more k points than those used in the relaxation calculations [$25\times25\times1$ for (100), $21\times21\times1$ for (110), and $30\times30\times1$ for (111) orientation]. The W substrates are modeled by 7-layer slabs for the W(100) and W(110) orientations, and 11-layer slabs are

TABLE IV. Magnetic moment of the overlayers as a function of their distances from the W substrate. Here 0 Å means that the overlayer is at the zero-force equilibrium position, while 0.5 and 1 Å mean that the overlayer is pulled up a distance of 0.5 and 1 Å from its equilibrium position, with the W atoms frozen.

	Magnetic moment (μ_B)		
	0.0 Å	0.5 Å	1.0 Å
Fe/5W(100)	1.89	2.91	3.09
Fe/5W(110)	2.45	2.87	3.00
Fe/7W(111)	2.30	2.90	3.13
Co/5W(100)	0.09	1.47	1.92
Co/5W(110)	1.40	2.02	2.11
Co/7W(111)	1.23	1.78	1.99
Ni/5W(100)	0.00	0.00	0.41
Ni/5W(110)	0.00	0.55	0.84
Ni/7W(111)	0.00	0.01	0.49

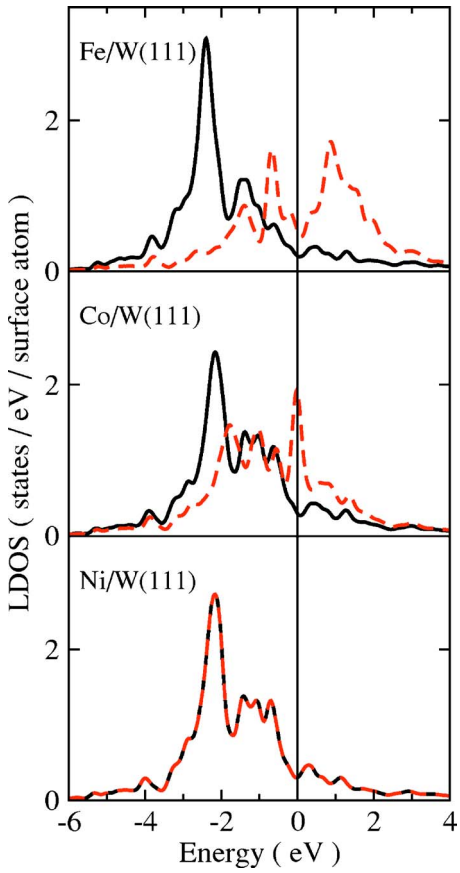

FIG. 1. (Color online) Local density of states of the overlayer atoms for Fe, Co, and Ni on W(111). The solid lines and dashed lines are for the majority and minority spins, respectively.

used for W(111). We will first look at the case of one monolayer of Fe, Co, and Ni on W(111), and the LDOS are shown in Fig. 1, in which the majority-spin LDOS (solid line) is compared with the minority-spin LDOS (dotted line). For the case of Ni, the majority and minority spins overlap since this system is not magnetic. For Fe and Co, there is a difference in the number of occupied electrons in the majority and minority spins, leading to the magnetic moments reported in the previous sections. The LDOS are actually rather generic in the three cases. In particular, the LDOS of the majority spin are quite similar for all three cases, and the *d* states in majority spin are mostly occupied, leading to a small majority spin DOS at the Fermi level. The difference in the magnetic properties of Fe, Co, and Ni comes from the difference in the occupation of the minority spin. Fe has the least number of electrons among the three elements; the minority-spin DOS is about half occupied in the *d* bands. In a bcc structural environment, half occupied *d* bands means a small DOS near the Fermi level (the physical picture is modified somewhat by the existence of surface states). In the case of Fe, even though the minority-spin LDOS is small because it is at the dip between two peaks (half band filling in bcc structure), it is still bigger than the majority-spin LDOS, leading to a moderate difference of DOS at the Fermi level. However, the total number of occupied electrons between the majority and minority spins is quite different, leading to a large magnetic moment.

Co has one more electron than Fe. The Fermi level is now at a peak of the minority-spin LDOS, corresponding to the maximum of the second peak of the double-peak DOS typically that of a bcc environment. This leads to a larger difference between majority- and minority-spin LDOS at the Fermi level. Since more electrons are now occupied in the minority spin (compared with Fe), there is a smaller difference between the number of occupied electrons in majority and minority spins, and therefore Co/W(111) has less total magnetization compared with Fe/W(111). Hence, Co/W(111) has a smaller total moment, but a larger difference between majority- and minority-spin DOS at E_f. If these systems are to be used as spin-polarized emission sources, Co/W(111) would be the better choice since it is the electrons with energy near the Fermi level that count in tunneling, even though Fe/W(111) has a larger total moment. For Ni, the minority-spin occupation is the same as that of the majority spin. In this case, the magnetization cannot survive the effect the nonmagnetic substrate.

In Fig. 2, we compare the LDOS of the Co atoms for one and two monolayers of Co on three different orientations of W. We first focus on the one-monolayer Co on W cases, the

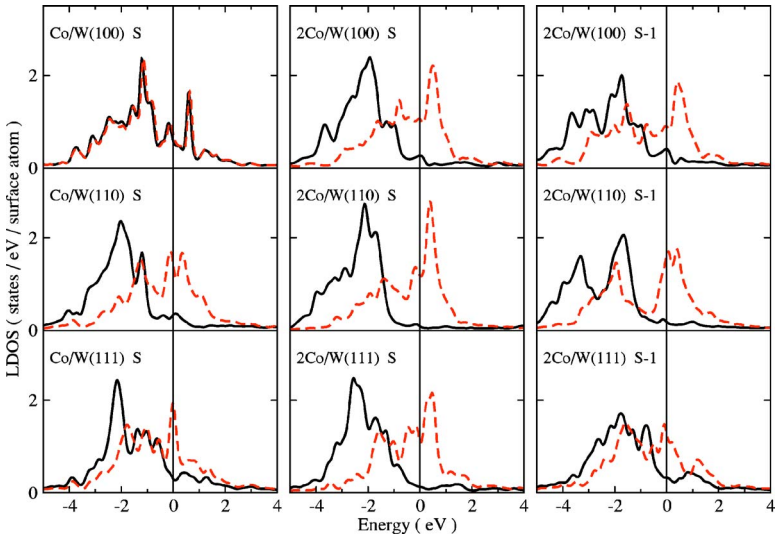

FIG. 2. (Color online) Comparing the local density of states of the overlayer Co atoms for one and two monolayers of Co on W(110), (100), and (111). The symbol "S" in the brackets indicates the top layer, and "S-1" indicates the subsurface Co layer when there are two monolayers. The solid lines and dashed lines are for the majority and minority spins, respectively.

LDOS, and hence the magnetic moment and the difference in LDOS at E_f differ significantly from one orientation to another. The (110) orientation has the largest magnetic moment as well as the largest difference in the LDOS at E_f. We note that the bandwidth of the d states is smaller in the (110) direction than the (100) and (111), a consequence of the smaller coupling of the Co states with the most compact W(110). This smaller coupling also manifests itself in other physical quantities: The Co layer is at 4.3 a.u. away from the W surface compared with 3 a.u. for the case of W(100), as well as the smallest heat of formation, as already explained in previous paragraphs.

We now compare the overlayer LDOS when there is one monolayer with the LDOS when there are two monolayers for the three different orientations of the W substrate. In Fig. 2, we found that the evolution of the LDOS as a function of the overlayer thickness and thus the total moment and the LDOS at E_f again depend very much on the surface orientation. The (110) orientation shows the least variation. When we compare the LDOS of the top layer when there are two monolayers with that of the single monolayer, we see that the former case has a larger splitting of the majority- and minority-spin states, leading to a higher magnetic moment. Despite these differences, the overall shapes of the LDOS for the monolayer and top layer of two monolayers are rather similar. This is consistent with our previous results, since the overlayer is at the largest distance away and shows the smallest interaction with the most compact (110) orientation of the substrate. On the other hand, the LDOS at the first monolayer differs significantly from that of the top layer when there are two layers on the (100) orientation, which has a maximum overlayer-substrate interaction. For the case of (111), there are also fairly significant changes.

For the cases of two monolayers, we note that the LDOS of the top and second layers of the minority spin look rather similar, while those of the majority spin show more differences. We observe more or less the same behavior for Fe. We do not have a very good explanation except that the minority-spin states in these systems tend to be more delocalized near the surface, leading to more similar LDOS when the DOS is projected to the different sites.

IV. SUMMARY

We have calculated the heat of formation and the magnetic moments of Fe, Co, and Ni on different orientations of the W surface. The surface magnetic properties are found to be strongly correlated with the cohesive properties and are orientation dependent. We are looking for thermodynamically stable and magnetically live thin films on W surfaces, with an eye on the possibility of using these systems as ultrathin-layer-coated tungsten field emission tips that give spin-polarized electrons. Maximum thermodynamic stability and large magnetic moment of the overlayer are found to be conflicting conditions. In general, we found that a large heat of formation, indicating strong interaction between overlayer and substrate, tends to diminish strongly the magnetic moment of the layer directly in contact with the nonmagnetic substrate. Additional monolayers quickly regain the magnetic moment in more compact orientations, because of the good screening effect of the layer in direct contact with the W substrate. The good screening also shields the second layer from direct bonding with the substrate, and the heat of formation also diminishes quickly. From a thermodynamical point of view, the system thus becomes marginally stable or metastable with respect to 3D island formation. However, there are systems like Co/W(111) in which the overlayers are thermodynamically stable and have reasonably large magnetic moments and large differences in the majority- and minority-spin DOS near E_f. There are cases, such as two layers of Fe on W(100) and three layers of Fe on W(111), that have the additional advantage of having a relatively low work function, which may be favorable for field emission.

We emphasize that a thermodynamically stable and ferromagnetic coating with a large difference in the DOS near E_f is just a plausible candidate as a spin-polarized field emitter tip. The polarization of the emitted electrons does not only depend on the LDOS near E_f. It depends also on the transverse component momentum of the electron states, the details of the wave function, and the details of the potential function near the surface when an external field is induced. These factors can be considered as a scattering problem. We have also restricted our calculations to a (1×1) surface unit cell. It is possible that antiferromagnetic or other spin configurations may have lower energies in these thin films, and to answer these questions, we have to use larger surface unit cells. It is possible that fluctuation is large in thin layers so that the Curie temperature is below room temperature. All these complex and interconnected factors have to be considered in the design of a serviceable spin-polarized field emission tip, and these will be the subject of further studies.

ACKNOWLEDGMENTS

We thank Dr. M. Altman for many discussions. This work was supported by National Science Council Grant Nos. NSC92-2112-M194-018, NSC92-2120-M194-002, and NSC92-2120-M194-003, by the Research Grant Council Hong Kong through Grant No. HKUST 6152/01P, and by a grant of computer time at the National Center for High-Performance Computing.

[1] Soon C. Hong, A. J. Freeman, and C. L. Fu, Phys. Rev. B **38**, 12156 (1988).
[2] Ruqian Wu and A. J. Freeman, J. Magn. Magn. Mater. **127**, 327 (1993).
[3] E. Vescovo, O. Rader, J. Redinger, S. Blugel, and C. Carbone, Phys. Rev. B **51**, 12418 (1995).
[4] S. Blügel, Phys. Rev. B **51**, R2025 (1995).
[5] See, for example, M. Pratzer, H. J. Elmers, M. Bode, O. Pietzsch, A. Kubetzka, and R. Wiesendanger, Phys. Rev. Lett. **87**, 127201 (2001); O. Pietzsch, A. Kubetzka, M. Bode, and R. Wiesendanger, *ibid.* **84**, 5212 (2000).
[6] R. Wiesendanger, I. V. Shvets, D. Burgler, G. Tarach, H. J. Guntherodt, J. M. D. Coey, and S. Graser, Science **255**, 583 (1992); S. Heinze, M. Bode, A. Kubetzka, O. Pietzsch, X. Nie, S. Blügel, and R. Wiesendanger, *ibid.* **288**, 1805 (2000); M. Bode, S. Heinze, A. Kubetzka, O. Pietzsch, M. Hennefarth, M. Getzlaff, R. Wiesendanger, X. Nie, G. Bihlmayer, and S. Blügel, Phys. Rev. B **66**, 014425 (2002); N. Berdunov, S. Murphy, G. Mariotto, and I. V. Shvets, Phys. Rev. Lett. **93**, 057201 (2004).
[7] P. Blaha, K. Schwarz, G. K. H. Madsen, D. Kvasnicka, and J. Luitz, WIEN2k, an augmented plane wave+local orbitals program for calculating crystal properties, Karlheinz Schwarz, Technical Universität, Wien, Austria, 2001, ISBN 3-9501031-1-2. We used version WIEN2k_05.1.
[8] D. J. Singh, *Plane Waves, Pseudopotentials and the LAPW Method* (Kluwer Academic, Dordrecht, 1996).
[9] W. Kohn and L. J. Sham, Phys. Rev. **140**, A1133 (1965).
[10] J. P. Perdew, K. Burke, and M. Ernzerhof, Phys. Rev. Lett. **80**, 891 (1998).
[11] X. Qian and W. Hübner, Phys. Rev. B **64**, 092402 (2001).
[12] X. Qian and W. Hübner, Phys. Rev. B **60**, 16192 (1999).
[13] U. Gradmann, in *Handbook of Magnetic Materials*, edited by K. H. J. Buschow (North-Holland, Amsterdam, 1993), Vol. 7, Chap. 1.
[14] P. E. Blochl, Phys. Rev. B **50**, 17953 (1994).
[15] G. Kresse and J. Hafner, Phys. Rev. B **47**, R558 (1993); **49**, 14251 (1994); G. Kresse and J. Furthmüller, Comput. Mater. Sci. **6**, 15 (1996); G. Kresse and J. Hafner, J. Phys.: Condens. Matter **6**, 8245 (1994).
[16] T. C. Leung, C. L. Kao, W. S. Su, Y. J. Feng, and C. T. Chan, Phys. Rev. B **68**, 195408 (2003).
[17] Y. Yamamoto and T. Miyokawa, J. Vac. Sci. Technol. B **16**, 2871 (1998).